

# Tumour genomic and microenvironmental heterogeneity for integrated prediction of 5-year biochemical recurrence of prostate cancer: a retrospective cohort study



Emilie Lalonde\*, Adrian S Ishkanian\*, Jenna Sykes, Michael Fraser, Helen Ross-Adams, Nicholas Erho, Mark J Dunning, Silvia Halim, Alastair D Lamb, Nathalie C Moon, Gaetano Zafarana, Anne Y Warren, Xianyue Meng, John Thoms, Michal R Grzadkowski, Alejandro Berlin, Cherry L Have, Varune R Ramnarine, Cindy Q Yao, Chad A Malloff, Lucia L Lam, Honglei Xie, Nicholas J Harding, Denise Y F Mak, Kenneth C Chu, Lauren C Chong, Dorota H Sendorek, Christine P'ng, Colin C Collins, Jeremy A Squire, Igor Jurisica, Colin Cooper, Rosalind Eeles, Melania Pintilie, Alan Dal Pra, Elai Davicioni, Wan L Lam, Michael Milosevic, David E Neal, Theodor van der Kwast, Paul C Boutros, Robert G Bristow

## Summary

**Background** Clinical prognostic groupings for localised prostate cancers are imprecise, with 30–50% of patients recurring after image-guided radiotherapy or radical prostatectomy. We aimed to test combined genomic and microenvironmental indices in prostate cancer to improve risk stratification and complement clinical prognostic factors.

**Methods** We used DNA-based indices alone or in combination with intra-prostatic hypoxia measurements to develop four prognostic indices in 126 low-risk to intermediate-risk patients (Toronto cohort) who will receive image-guided radiotherapy. We validated these indices in two independent cohorts of 154 (Memorial Sloan Kettering Cancer Center cohort [MSKCC] cohort) and 117 (Cambridge cohort) radical prostatectomy specimens from low-risk to high-risk patients. We applied unsupervised and supervised machine learning techniques to the copy-number profiles of 126 pre-image-guided radiotherapy diagnostic biopsies to develop prognostic signatures. Our primary endpoint was the development of a set of prognostic measures capable of stratifying patients for risk of biochemical relapse 5 years after primary treatment.

**Findings** Biochemical relapse was associated with indices of tumour hypoxia, genomic instability, and genomic subtypes based on multivariate analyses. We identified four genomic subtypes for prostate cancer, which had different 5-year biochemical relapse-free survival. Genomic instability is prognostic for relapse in both image-guided radiotherapy (multivariate analysis hazard ratio [HR] 4.5 [95% CI 2.1–9.8];  $p=0.00013$ ; area under the receiver operator curve [AUC] 0.70 [95% CI 0.65–0.76]) and radical prostatectomy (4.0 [1.6–9.7];  $p=0.0024$ ; AUC 0.57 [0.52–0.61]) patients with prostate cancer, and its effect is magnified by intratumoral hypoxia (3.8 [1.2–12];  $p=0.019$ ; AUC 0.67 [0.61–0.73]). A novel 100-loci DNA signature accurately classified treatment outcome in the MSKCC low-risk to intermediate-risk cohort (multivariate analysis HR 6.1 [95% CI 2.0–19];  $p=0.0015$ ; AUC 0.74 [95% CI 0.65–0.83]). In the independent MSKCC and Cambridge cohorts, this signature identified low-risk to high-risk patients who were most likely to fail treatment within 18 months (combined cohorts multivariate analysis HR 2.9 [95% CI 1.4–6.0];  $p=0.0039$ ; AUC 0.68 [95% CI 0.63–0.73]), and was better at predicting biochemical relapse than 23 previously published RNA signatures.

**Interpretation** This is the first study of cancer outcome to integrate DNA-based and microenvironment-based failure indices to predict patient outcome. Patients exhibiting these aggressive features after biopsy should be entered into treatment intensification trials.

**Funding** Movember Foundation, Prostate Cancer Canada, Ontario Institute for Cancer Research, Canadian Institute for Health Research, NIHR Cambridge Biomedical Research Centre, The University of Cambridge, Cancer Research UK, Cambridge Cancer Charity, Prostate Cancer UK, Hutchison Whampoa Limited, Terry Fox Research Institute, Princess Margaret Cancer Centre Foundation, PMH-Radiation Medicine Program Academic Enrichment Fund, Motorcycle Ride for Dad (Durham), Canadian Cancer Society.

**Copyright** © Lalonde et al. Open Access article distributed under the terms of CC BY.

## Introduction

Every year, almost 900 000 men worldwide are diagnosed with prostate cancer, and 250 000 men die annually from the disease.<sup>1</sup> Most cases are localised cancers, which are stratified into low-risk, intermediate-risk and high-risk groups on the basis of their prostate cancer-specific mortality.<sup>2</sup> These clinical prognostic groups are based on

pretreatment PSA (PSA), biopsy-based pathological Gleason scores, and TNM staging descriptors, such as the National Comprehensive Cancer Network classification system.<sup>3</sup>

Low-risk patients (ie, those with Gleason scores  $\leq 6$ , PSA concentrations  $<10$  ng/mL, or T1–T2a) can be offered active surveillance, sparing them the toxic effects

Lancet Oncol 2014; 15: 1521–32

Published Online

November 13, 2014

[http://dx.doi.org/10.1016/S1470-2045\(14\)71021-6](http://dx.doi.org/10.1016/S1470-2045(14)71021-6)

See [Comment](#) page 1419

\*These authors contributed

equally

Informatics and Bio-Computing Program, Ontario Institute for Cancer Research, Toronto, ON, Canada

(E Lalonde MSc,

N C Moon MMath,

M R Grzadkowski BMath,

C Q Yao MSc, H Xie MMath,

N J Harding PhD, D Y F Mak PhD,

K C Chu PhD, L C Chong BCS,

D H Sendorek BSc, C P'ng BSc,

Prof P C Boutros PhD); Sylvester Comprehensive Cancer Center,

Miller School of Medicine,

University of Miami, Miami,

USA (A S Ishkanian MD);

Department of Medical

Biophysics (E Lalonde,

V R Ramnarine BCS, C Q Yao,

Prof I Jurisica PhD,

Prof P C Boutros,

Prof R G Bristow MD)

Department of Radiation

Oncology (M Fraser PhD,

G Zafarana PhD, J Thoms MD,

A Berlin MD, A D Pra MD,

M Milosevic MD,

Prof T van der Kwast MD,

Prof R G Bristow), and

Department of Pharmacology

and Toxicology

(Prof P C Boutros), University of

Toronto, Toronto, ON, Canada;

Princess Margaret Cancer

Centre, University Health

Network, Toronto, ON, Canada

(J Sykes MMath, M Fraser,

G Zafarana, X Meng MSc,

J Thoms, A Berlin, V R Ramnarine,

K C Chu, Prof I Jurisica,

M Pintilie MSc, A D Pra,

M Milosevic, Prof R G Bristow);

Uro-Oncology Research Group

(H Ross-Adams PhD,

A D Lamb FRCS,

Prof D E Neal MD) and Bioinformatics Core (M J Dunning PhD, S Halim MSc), Cancer Research UK Cambridge Institute, University of Cambridge, Cambridge, UK; Department of Urology, Cambridge Biomedical Campus, Addenbrooke's Hospital, Cambridge, UK (A D Lamb, Prof D E Neal); Research and Development, GenomeDx Biosciences, Vancouver, BC, Canada (N Erho MSc, L L Lam BSc, E Davicioni PhD); Department of Pathology, Addenbrooke's Hospital, Cambridge, UK (A Y Warren FRCPath); Department of Pathology, Laboratory Medicine Program, University Health Network, Toronto, ON, Canada (C L Have BSc, Prof T van der Kwast); Vancouver Prostate Centre and Department of Urological Sciences, University of British Columbia, Vancouver, BC, Canada (V R Ramnarine, Prof C C Collins PhD); Department of Integrative Oncology, BC Cancer Research Centre, Vancouver, BC, Canada (C A Malloff MSc, Prof W L Lam PhD); Center for Addiction and Mental Health, Toronto, ON, Canada (D Y F Mak); Department of Pathology and Forensic Medicine, University of São Paulo at Ribeirão Preto, Ribeirão Preto, Brazil (Prof J A Squire PhD); Division of Genetics and Epidemiology, The Institute of Cancer Research, Sutton, UK (C Cooper PhD, Prof R Eeles PhD); Department of Biological Sciences and School of Medicine, University of East Anglia, Norwich, UK (C Cooper); Royal Marsden National Health Service Foundation Trust, London, UK (Prof R Eeles); and Department of Radiation Oncology, Bern University Hospital, Bern, Switzerland (A D Pra)

Correspondence to: Robert G Bristow, Departments of Medical Biophysics and Radiation Oncology, University of Toronto, Toronto, ON M5G 2M9, Canada rob.bristow@rmp.uhn.on.ca

See Online for appendix

of treatment. By contrast, patients with intermediate risk (Gleason scores of 7, PSA concentrations of 10–20 ng/mL, or T2b-c) and high risk or locally advanced (Gleason scores  $\geq 8$ , prostate specific antigen concentrations  $\geq 20$  ng/mL, or T3/4) prostate cancer often undergo radical prostatectomy or image-guided radiotherapy, or receive intensified regimens adding adjuvant androgen deprivation therapy or novel systemic drugs to prevent progression to metastatic castration-resistant prostate cancer. However, use of treatment intensification for individual patients is imprecise: 30–50% of patients have biochemical relapse despite radical prostatectomy or image-guided radiotherapy.<sup>4,5</sup> Furthermore, nearly 20% of intermediate-risk patients have biochemical failure within 18 months of primary local therapy (ie, rapid failure). Such failure might be due to pre-existing occult metastatic disease, because rapid biochemical failure is a surrogate for prostate-cancer-specific mortality.<sup>6,7</sup> The basis of this interpatient clinical heterogeneity has not been clinically resolved.<sup>8,9</sup>

A signature to classify patients as potential responders or non-responders to local therapy would have great clinical use if it was treatment-independent (ie, effective both for patients undergoing radical prostatectomy or image-guided radiotherapy) and could be done on initial diagnostic biopsies. Such a signature could triage patients at greatest risk of failure into clinical trials for treatment intensification and justify potential added toxic effects.<sup>7,10</sup> DNA copy number alterations in *PTEN*, *NKX3-1*, *MYC*, and *STAR* are associated with adverse prognosis,<sup>11,12</sup> and RNA-based gene signatures might differentiate indolent and non-indolent, lethal prostate cancer.<sup>13–15</sup> *TMPRSS2-ERG* fusion status does not predict prognosis after radical prostatectomy or image-guided radiotherapy.<sup>16,17</sup> Importantly, tumour cells exist within a heterogeneous tumour microenvironment with dynamic gradients of hypoxia that have been linked to metastatic potential.<sup>9,18</sup> Indeed, patients with prostate cancer with hypoxic tumours rapidly fail treatment (eg, within 2 years) after radical prostatectomy or image-guided radiotherapy.<sup>19,20</sup> Up to now, the interplay of genomic instability and tumour microenvironment in modulation of treatment outcome has been unexplored. We therefore aimed to develop clinically relevant prognostic indices, with use of integrated tumour DNA and microenvironmental indices, to robustly predict patient outcome.

## Methods

### Study design and patients

Our training (Toronto) cohort for generation of biopsy-based signatures consisted of pre-image-guided radiotherapy, clinically-staged patients with prostate cancer, who were classified as low-risk or intermediate-risk on the basis of National Comprehensive Cancer Network guidelines (appendix).<sup>3</sup> To validate our findings, we used copy number alteration profiles from two

cohorts of clinically staged (ie, similar to pre-image-guided radiotherapy patients) low-risk to high-risk radical prostatectomy patients (Memorial Sloan Kettering Cancer Center cohort [MSKCC] and Cambridge cohorts; appendix).<sup>8</sup> The radical prostatectomy cohorts were considered both separately and together. We defined copy number alteration profiles relative to the hg19 human genome build.

DNA was extracted from pretreatment biopsies that consisted of at least 70% tumour cells as estimated by a pathologist (TvdK), and a custom array was used to detect copy number alterations.<sup>12</sup> Intraglandular measurements of partial oxygen pressure were taken before radiotherapy with an ultrasound-guided transrectal needle piezoelectrode.<sup>20</sup>

We developed four prognostic indices and validated them for prediction of biochemical relapse (appendix). The appendix provides an overview of our approach to develop treatment-independent, integrated prognostic indices. First, we identified unique genomic subtypes with use of unsupervised hierarchical clustering. Second, we used the percentage of a patient's genome harbouring copy number alterations (percent genome alteration) as a surrogate for genomic instability, and assessed this proportion together with tumour hypoxia. Third, we undertook supervised machine learning with a random forest<sup>21</sup> to develop a statistical model, resulting in a DNA signature, which classified patients at risk of biochemical relapse on the basis of their copy-number profiles. We compared the resulting signature with published RNA-based signatures.

### Statistical analysis

Our main aim was the development of a set of prognostic measures capable of stratifying patients for risk of biochemical relapse (defined as an increase in concentration of prostate-specific antigen of at least 2 ng/mL above the post-radiation nadir value for image-guided radiotherapy patients and, for radical prostatectomy patients, as two consecutive concentration values  $>0.2$  ng/mL or triggered salvage radiotherapy<sup>22,23</sup>) 5 years after primary treatment. Our secondary aim was the status at 18 months. We assessed prognosis for biochemical relapse by the area under the receiver operator curve (AUC), C-index analysis, and Cox proportional hazard regression models. We modelled indices with univariate and multivariate analyses, with multivariate analyses correcting for Gleason score and pre-treatment concentrations of PSA (and clinical T stage during assessment of high-risk patients; appendix). The appendix shows full C-index analyses for each biomarker. We used two-sided non-parametric tests to compare patient subsets. We applied multiple-testing correction with the Benjamini-Hochberg or Bonferroni method, as indicated. We did all bioinformatic and statistical analyses in the R statistical environment (version 3.0.2).

### Role of the funding source

The funders of the study had no role in study design, data collection, data analysis, data interpretation, or writing of the report. All authors had full access to all the data in the study and the corresponding author had final responsibility for the decision to submit for publication.

### Results

We used information derived from 126 pre-image-guided radiotherapy biopsies (Toronto cohort) and did initial validation with 154 radical prostatectomy specimens (MSKCC cohort). We obtained a secondary independent cohort of 117 radical prostatectomy specimens for further validation of putative biomarkers (Cambridge cohort). Clinical characteristics of the patients are listed in the appendix (pp 11–12). We focused on clinically-matched validation cohorts containing low-risk and intermediate-risk patients (n=210) who might need treatment intensification beyond local therapy alone, but also considered all patients with localised disease who might be candidates for intensification or de-intensification (full validation cohort n=271). 5-year biochemical relapse-free survival of the three study cohorts were broadly similar (appendix pp 36–39). Pretreatment PSA was prognostic in image-guided radiotherapy patients, whereas pretreatment Gleason score, T category, and PSA were all prognostic in the full MSKCC and Cambridge cohorts (table 1).

Our initial analyses showed that Toronto and MSKCC cohorts showed extensive genomic heterogeneity, even for patients who were low-risk or intermediate-risk, or had Gleason scores of 6 or 7 (appendix pp 13, 40–43). The most recurrent copy number alterations in either cohort were 8p amplifications and 8q deletions, in addition to deletions of 16q23·2 and 6q15 (harbouring *MAF* and *MAP3K7*; table 2), which have been noted in aggressive tumours.<sup>24</sup> We established the frequency of copy number alterations for a set of genes putatively prognostic for adverse outcomes, selected from our previous studies and the literature, in the Toronto image-guided radiotherapy biopsies (appendix p 44). Despite low-risk or intermediate-risk classification, 76 (60%) of 126 patients had copy number alterations in at least two adverse prognosis genes. We noted this variability across the genome, suggesting that genomically defined subtypes of prostate cancer might be obtained from biopsies.

Unbiased hierarchical clustering in the Toronto cohort (appendix pp 45–46) showed four localised prostate cancer subtypes with distinct genomic profiles: subtype 1 (characterised by gain of chromosome 7), subtype 2 (deletion of 8p and gain of 8q), subtype 3 (loss of 8p and 16q), and subtype 4 (so-called quiet genomes due to few genomic alterations). Subtypes 2 and 3 share many common genetic alterations (504 genes altered in >25% of patients in both subtypes), but  $\chi^2$  tests showed eight regions that differed significantly, including gain of 8q in

	Toronto		MSKCC full		Cambridge full	
	Univariate	Multivariate	Univariate	Multivariate	Univariate	Multivariate
<b>Data for each prognostic clinical variable*</b>						
Gleason score						
7 vs 5–6	1·0 (0·44–2·4; 0·95)	1·0 (0·44–2·5; 0·92)	3·4 (1·5–8·0; 0·0044)	2·8 (1·2–6·71; 0·019)	6·2 (0·82–47; 0·078)	5·6 (0·74–43; 0·95)
8–9 vs 5–6	NA	NA	7·3 (2·9–18; <0·0001)	4·9 (1·8–131; 0·0015)	8·1 (0·85–78; 0·069)	5·7 (0·58–56; 0·14)
PSA (continuous)†	1·2 (1·1–1·3; 0·0012)	NA	1·006 (1·003–1·009; 0·00030)	NA	1·1 (1·0–1·2; 0·063)	NA
T category						
T2 vs T1‡	0·82 (0·39–1·7; 0·60)	0·86 (0·40–1·8; 0·69)	NA	NA	NA	NA
T3 vs T1–2‡	NA	NA	9·2 (4·1–21; <0·0001)	6·1 (2·6–14; <0·0001)	2·8 (1·0–7·8; 0·50)	3·6 (1·2–11; 0·024)
National Comprehensive Cancer Network classification						
Intermediate vs low risk	1·4 (0·43–4·7; 0·57)	NA	2·5 (0·80–7·91; 0·12)	NA	2·2 (0·28–18; 0·45)	NA
High vs low risk	NA	NA	12·6 (4·3–37; <0·0001)	NA	6·9 (0·88–55; 0·66)	NA
<b>Data for dichotomised and continuous PGA§</b>						
≥7·49 vs <7·49	4·2 (2·0–8·9; 0·00019)	4·5 (2·1–9·8; 0·00013)	4·5 (2·3–8·9; <0·0001)	3·4 (1·6–7·2; 0·0011)	3·8 (1·4–9·9; 0·0075)	3·2 (1·1–9·0; 0·029)
Continuous	1·05 (1·03–1·08; <0·0001)	1·06 (1·03–1·09; 0·00019)	1·08 (1·04–1·13; 0·0098)	1·05 (1·0–1·1; 0·065)	1·09 (1·0–1·2; 0·0020)	1·08 (1·0–1·1; 0·0012)
AUC	0·71 (0·66–0·77)	0·70 (0·65–0·76)	0·49 (0·44–0·54)	0·82 (0·76–0·88)	0·70 (0·63–0·77)	0·71 (0·58–0·73)
C index	0·72 (0·64–0·81)	0·63 (0·60–0·79)	0·60 (0·48–0·72)	0·76 (0·63–0·80)	0·65 (0·50–0·70)	0·72 (0·61–0·84)

Data are hazard ratio (95% CI) or hazard ratio (95% CI; p-value). 5-year biochemical relapse rate was used in the Cox proportional hazard models except for the Cambridge cohort in which 18-month biochemical relapse rate was used. IGRT=image-guided radiotherapy. MSKCC=Memorial Sloan Kettering Cancer Center. NA=not applicable. PGA=percentage of genome alteration. AUC=area under the receiver operator curve. \*Data from Cox proportional hazard models are shown for each prognostic clinical variable in the univariate and multivariate setting for each full cohort. Multivariate models include Gleason score, prostate-specific antigen, and T category only (National Comprehensive Cancer Network classification is not included). The multivariate models show the covariates and levels used for multivariate analysis of biomarkers throughout the study. †PSA is stratified at 10 ng/mL because it fails the proportional hazards assumption. ‡For the Toronto-IGRT cohort, in which there were only low-risk to intermediate-risk patients, we compared T2–T3 patients, whereas for the radical prostatectomy cohorts, we compared T3 patients with T1–2 patients. §Data are provided for dichotomised and continuous PGA in each cohort, on the basis of Cox proportional hazard models including only the marker of interest (univariate) and models including relevant clinical covariates as shown in the table (multivariate). The AUC and C index are provided for the continuous PGA values.

**Table 1: Biomarker summary for each prognostic clinical variable and for PGA in each cohort**

	Type	IGRT rank	MSKCC rank	Genes in region*
8p21.3	Del	1	5	PEBP4, RHOBTB2, TNFRSF10B, TNFRSF10C, TNFRSF10D, TNFRSF10A, CHMP7, LOXL2, ENTPD4
8p11.22	Del	42	1	FGFR1, C8orf86
8p23.1	Del	2	2	DEFB103A, DEFB103B, SPAG11B, DEFB104A, DEFB104B, DEFB106A, DEFB106B, DEFB105A, DEFB105B, DEFB107A, DEFB107B, SPAG11A, DEFB4
8p22.1	Del	3	3	NKX3-1, STC1
8q24.3	Amp	29	78	COL22A1 KCNK9 TRAPPC9 CHRAC1 EIF2C2 PTK2 DENND3 SLC45A4 GPR20 PTP4A3 FLJ43860 TSNARE1 BAI1 ARCJRK PSCA LY6K C8orf55 SLURP1 LYPD2 LYNX1 LY6D GML
8q21.2	Amp	7	167	REXO1L1
16q22.2	Del	16	9	HP, HPR, TXNL4B, DHX38, PMFBP1, ZFH3
16q23.2	Del	6	52	WWOX, MAF, DYNLRB2, CDYL2, C16orf61, CENPN, ATMIN, C16orf46, GCSH, PKD1L2, BCMO1, GAN, CMIP
6q15	Del	13	17	MAP3K7, BACH2
15q11	Del	16	60	LRCH1 ESD HTR2A SUCLA2 NUDT15 MED4 ITM2B RB1 P2RY5 RCBTB2 CYSLTR2 FNDC3A MLNR CDADC1 CAB39L SETDB2 PHF11 RCBTB1 ARL11 EBPL KPNA3 C13orf1 TRIM13 KCNRG

Chromosomal regions assessed for recurrence in the Toronto and MSKCC cohorts. Genes with most copy number alterations or those with known or putative cancer associations are shown. IGRT=image-guided radiotherapy. MSKCC=Memorial Sloan Kettering Cancer Center. \*Genes with most copy number alterations or those with known or putative cancer associations.

Table 2: Most recurrently aberrant regions

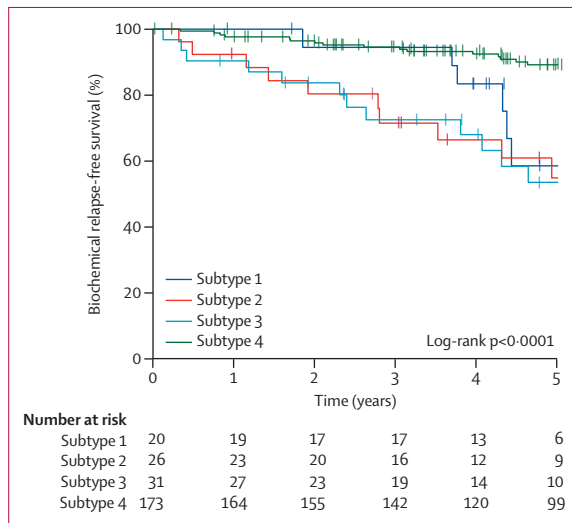


Figure 1: Kaplan-Meier analysis of biochemical-relapse free survival for patients stratified by tumour subtype

subtype 2 and 16q deletion in subtype 3 (appendix p 14). All four subtypes were confirmed in the MSKCC radical prostatectomy cohort and were not associated with *TMPRSS2-ERG* fusion, Gleason score, or T category (appendix pp 15–17, 47–48).

In a pooled analysis of low-risk and intermediate-risk patients (using the Toronto and MSKCC cohorts; 250 patients), the four genomic subtypes of localised prostate cancer had significantly different prognoses, even after adjustment for clinical variables (figure 1,

appendix pp 15–19, 43–49). Patients classified as subtype 4 had a significantly better prognosis compared with those with other subtypes (figure 1). Biochemical relapse-free survival at 5 years was 58% (95% CI 37–92) for subtype 1, 55% (37–81) for subtype 2, 53% (37–78) for subtype 3, and 89% (84–94) for subtype 4. Subtype 1 seems to be characterised by increased relapse after 3 years rather than increased risk at all times, but larger cohorts are needed to clarify this finding. These subtypes are prognostic for biochemical recurrence by 18 months (log-rank p value 0.0024, low-risk to intermediate-risk cohort), which is associated with increased prostate-cancer-specific mortality.<sup>6,7</sup> Indeed, in the Toronto cohort, being subtype 2 was associated with significantly worse overall survival than being in subtype 4 (HR 4.2 (95% CI 1.2–15; Wald  $p=0.03$ ; appendix p 19).

The excellent prognosis of so-called quiet subtype 4 suggested that genome-wide instability might be prognostic in itself. With the percentage of the genome showing a copy number alteration as a proxy for genomic instability, we noted interpatient variability in percentage of genome alteration ranging from 0–52% in the Toronto cohort, to 0–34% in the MSKCC cohort, and 0–28% in the Cambridge cohort. Percentage of genome alteration was independent of Gleason score, T category, and PSA in all cohorts (figures 2A–C). Indeed, individual Gleason score-6 tumours had a higher percentage of genome alteration than did some Gleason score 4+3 tumours (figure 2A), suggesting that percentage of genome alteration refines biological description even in tumours of mainly pattern 4. As expected, based on previous findings, the percentage of genome alteration was increased in patients with prognostic *CHD1* deletions (appendix p 50).<sup>25</sup>

Percentage of genome alteration was strongly prognostic, independent of clinical covariates, as previously reported.<sup>26</sup> Every 1% increase in percentage of alteration led to a 5–8% decrease in 5-year biochemical relapse-free survival (C-index 0.60–0.72; appendix pp 20–21). To classify the likelihood of clinical failure on the basis of percentage of genome alteration, we set the upper tertile of 7.49% from the Toronto cohort as the lower bound threshold, which efficiently stratified patients who underwent either image-guided radiotherapy (multivariate analysis HR for biochemical relapse 4.5 [95% CI 2.1–9.8]; Wald  $p=0.00013$ ) or radical prostatectomy (eg, pooled radical prostatectomy low-risk to intermediate-risk cohort: multivariate analysis HR for biochemical relapse 4.0 [1.6–9.7]; Wald  $p=0.0024$ ; figure 3A–C). These results are threshold-independent (appendix p 51). The HR for the pooled radical prostatectomy full (ie, low, intermediate, and high-risk) cohort at 5 years was 2.7 (95% CI 1.5–4.8;  $p=0.0024$ ; AUC 0.57 [95% CI 0.52–0.61]). Percentage of genome alteration stratifies patients at risk of rapid failure consistent with occult metastases, and was increased in

the primary tumours of patients who developed metastases compared with in those who did not and had a follow-up time of at least 5 years (median 9.2% [IQR 3.6–13] vs 2.8% [0.33–6.8];  $p=0.0043$  pooled Toronto and MSKCC cohorts, two-sided Mann-Whitney  $U$  test; appendix pp 52–54).

The median percentage of genome alteration differed significantly among our genomic subtypes, with subtypes 1 and 4 having the highest (12% [IQR 8.9–16]) and lowest (1.3% [0.16–3.2]) median percentages, respectively (appendix p 55). After the addition of percentage of genome alteration to the multivariate Cox proportional hazard model for subtypes, only subtypes 2 and 3 remained prognostic, suggesting that their prognostic ability stems from both specific genetic aberrations and general genomic instability (appendix p 18).

Hypoxia is an important aspect of cancer metabolism and in itself can be prognostic in patients with prostate cancer.<sup>19,20</sup> We used three hypoxia RNA signatures that have been validated in other tumour types to estimate hypoxia within the pooled radical prostatectomy mRNA cohorts (108 MSKCC patients and 110 Cambridge patients; table 3 and figure 4A–C; appendix p 22).<sup>27–29</sup> None of these signatures were univariately prognostic, nor were they related to Gleason score, PSA, T category, or percentage of genome alteration (appendix 56–59). However, when we separated patients into four groups on the basis of high versus low percentage of genome alteration and high versus low hypoxia values, we found that hypoxia increased the prognostic accuracy of the percentage genome alteration for risk of biochemical relapse. Patients with a high percentage of alteration and high hypoxia have the worst prognosis, whereas those with high hypoxia alone (low percentage of alteration) responded well after radical prostatectomy (figure 4A–C, appendix pp 23–24, 60–61).

To validate this finding, we used the Toronto cohort because the biobanking of frozen biopsies was completed with simultaneous and direct assessment of tumour hypoxia at the same intraprostatic locale.<sup>20</sup> This cohort therefore contained direct measurements of hypoxia denoted by patient-specific values for proportion of oxygen measurements less than 20 mm Hg (HP20; appendix p 25).<sup>20</sup> The median HP20 in our cohort was 81% (range 64–93). Although previous findings in a larger cohort have shown that hypoxia was independently prognostic of image-guided-radiotherapy outcome, our results did not show any significant association between median HP20 and increased biochemical-free survival (log-rank  $p=0.13$ ; appendix p 62).<sup>20</sup> Directly measured HP20 values were not related to the clinical covariates, genomic subtype, percentage of genome alteration, or with any individual copy number alteration, appendix pp 63–65), supporting a unique role in tumour biology of prostate cancer. We again noted that patients with a low percentage of genome alteration and low hypoxia had the best

outcome (biochemical relapse-free survival at 5 years was 93%), whereas those with high levels of both measures had the worst (49%; figure 4D). Moreover, we recorded a statistically significant interaction between

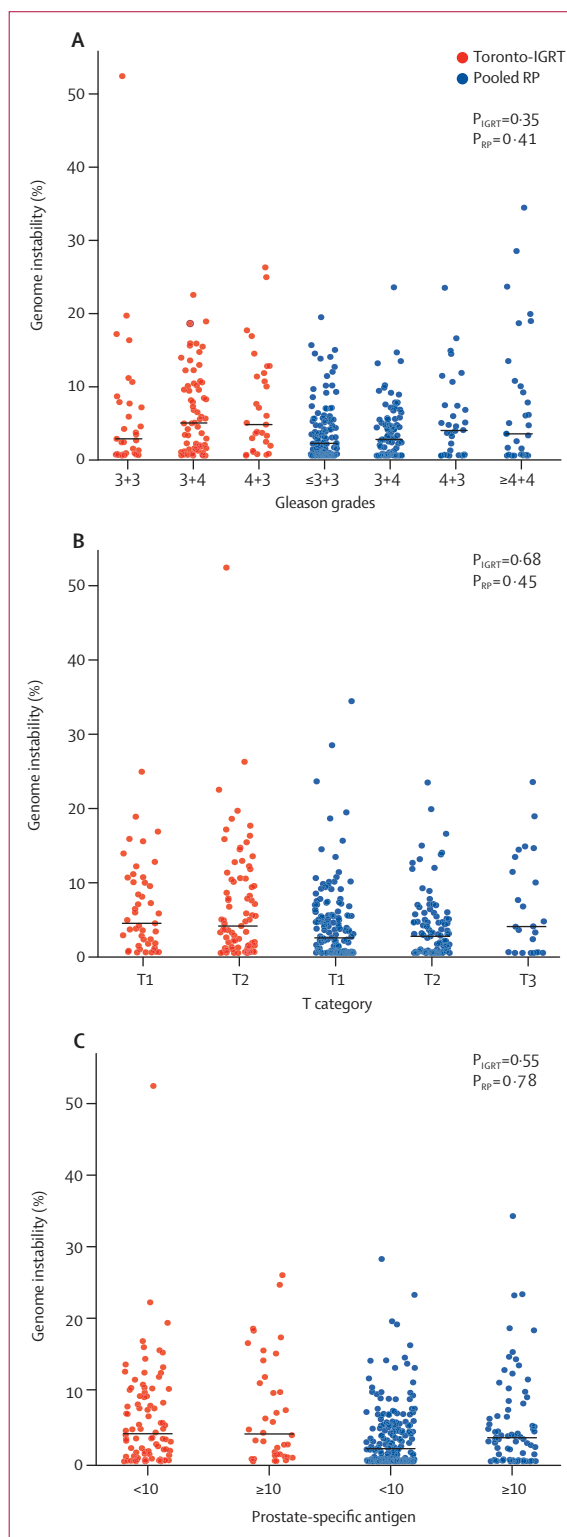


**Figure 2: Genomic instability (PGA) as an independent prognostic factor in patients with prostate cancer**

PGA is not a proxy for Gleason grade (A), clinical T category (B), or PSA (C;  $n=336$ , Toronto IGRT, Memorial Sloan Kettering Cancer Center, and Cambridge low-risk to intermediate-risk National Comprehensive Cancer Network classification risk groups combined).  $p$  values were obtained by two-tailed Kruskal-Wallis tests (A) and Mann-Whitney tests (B–C). Horizontal lines show median PGA values per group. IGRT=image-guided radiotherapy. RP=radical prostatectomy.

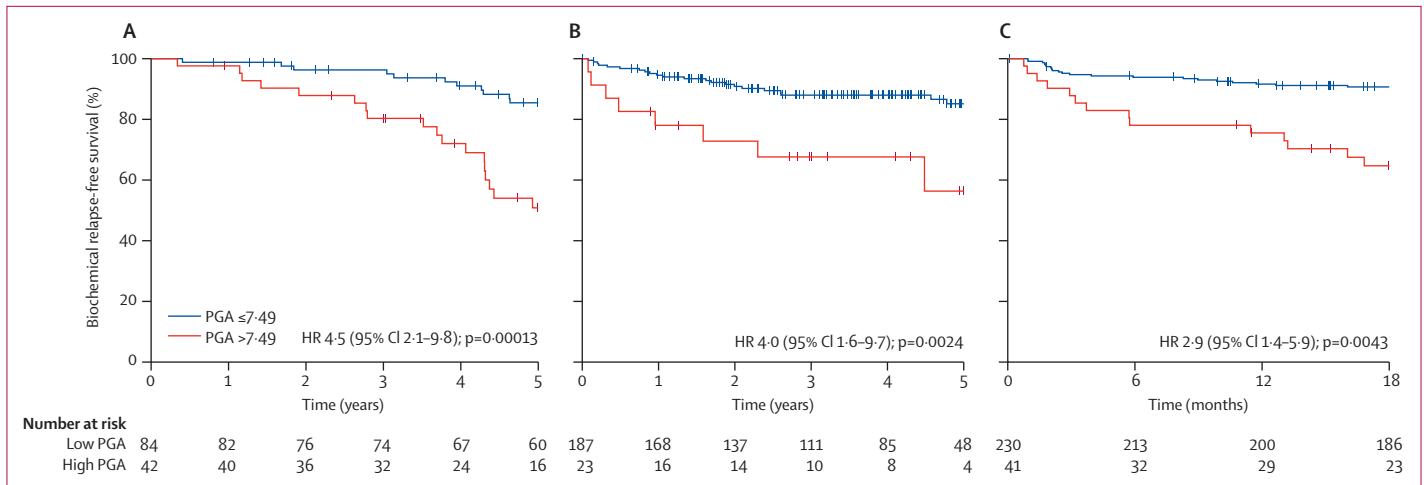


**Figure 3:** Kaplan-Meier analysis of PGA as a prognostic factor for biochemical treatment failure in image-guided radiotherapy patients (A) and those undergoing radical prostatectomy in the low-risk and intermediate-risk group (B) and the full group (C) PGA=percentage of genome alteration. HR=hazard ratio.

	Toronto cohort (HP20)	Pooled radical prostatectomy full cohort		
		Buffa RNA signature	West RNA signature	Winter RNA signature
+/- vs -/-*	11 (2.4-47; 0.0018)	2.3 (1.1-4.8; 0.031)	5.3 (1.8-16; 0.0027)	2.6 (1.1-5.9; 0.025)
AUC	0.67 (0.61-0.73)	0.58 (0.53-0.64)	0.59 (0.54-0.65)	0.53 (0.47-0.58)
C index	0.67 (0.59-0.75)	0.62 (0.54-0.71)	0.65 (0.58-0.73)	0.64 (0.55-0.73)

Data are hazard ratio (95% CI; p value) or hazard ratio (95% CI). Hazard ratios were not adjusted for clinical variables and the pooled radical prostatectomy cohorts are shown for all three RNA hypoxia signatures. AUC=area under the receiver operator curve. \*The Cox proportional hazard model was fit with four levels (percentage of genome alteration status/hypoxia status: +/+, +/-, -/+, and -/-, whereby +/- patients had a high percentage of genome alteration and high hypoxia, +/- patients had high a high percentage of genome alteration and low hypoxia, etc), with -/- patients used as the baseline group.

**Table 3: Data for patients stratified by hypoxia**

percentage of genome alteration and hypoxia (unadjusted HR for biochemical relapse 3.8 [95% CI 1.2-12]; Wald p=0.019; appendix pp 26-27) when used as a combined prognostic index. Again, patients whose tumour solely showed hypoxia, but not genome alteration, fared better than expected for patients with hypoxic tumours after image-guided radiotherapy, suggesting that cohorts of patients with high hypoxia and a high percentage of genome alteration could benefit from treatment intensification.

Because specific genes (figure 1), general genomic instability (figures 2, 3), and tumour microenvironment (figure 4) all play a part in determination of patient prognosis, we postulated that a supervised machine learning approach would capture the complex and

unknown interactions between genes underlying these events. Using a random forest<sup>21</sup> classifier trained on the Toronto cohort, we developed a biopsy-driven prognostic signature that predicts biochemical failure and could guide clinical decisions before, and independent of, treatment (appendix pp 66-67). The resulting 100-loci (276 genes) DNA signature was validated in two independent cohorts (figure 5; appendix 28-30, 68-77). We first verified the signature in the independent low-risk and intermediate-risk MSKCC cohort, in which it predicted biochemical relapse with an area under the curve of 0.74 (95% CI 0.65-0.83). This signature is more effective than clinical variables for prediction of biochemical relapse (table 4; appendix pp 28, 68-69). 58% (95% CI 35-96) of patients in the MSKCC low-risk to intermediate-risk groups who were classified as poor prognosis were biochemical relapse-free at 5 years, compared with 89% (85-96) for those classified as good prognosis, and this difference remained significant after adjustment for clinical covariates (multivariate analysis HR for biochemical relapse 6.1 [95% CI 2.0-19]; Wald p=0.0015; appendix pp 29, 70). Importantly, our signature effectively identified patients at risk of relapse within 18 months in the full MSKCC cohort, despite not including any high-risk patients in the initial training cohort (3.3 [1.1-10]; Wald p=0.038). We validated this early-failure effect in a second independent Cambridge cohort (2.8 [1.7-9.4]; Wald p=0.050; appendix pp 30, 70). The HR for the combined cohort is 2.9 (95% CI 1.4-6.0; p=0.039; AUC 0.68 [95% CI 0.63-0.73]). The signature is independent of clinical covariates and might identify candidates for both treatment intensification and de-intensification protocols because it can identify patients with a Gleason score 7 who will have biochemical relapse within 18 months (HR for relapse 2.8 [95% CI 1.2-6.7];

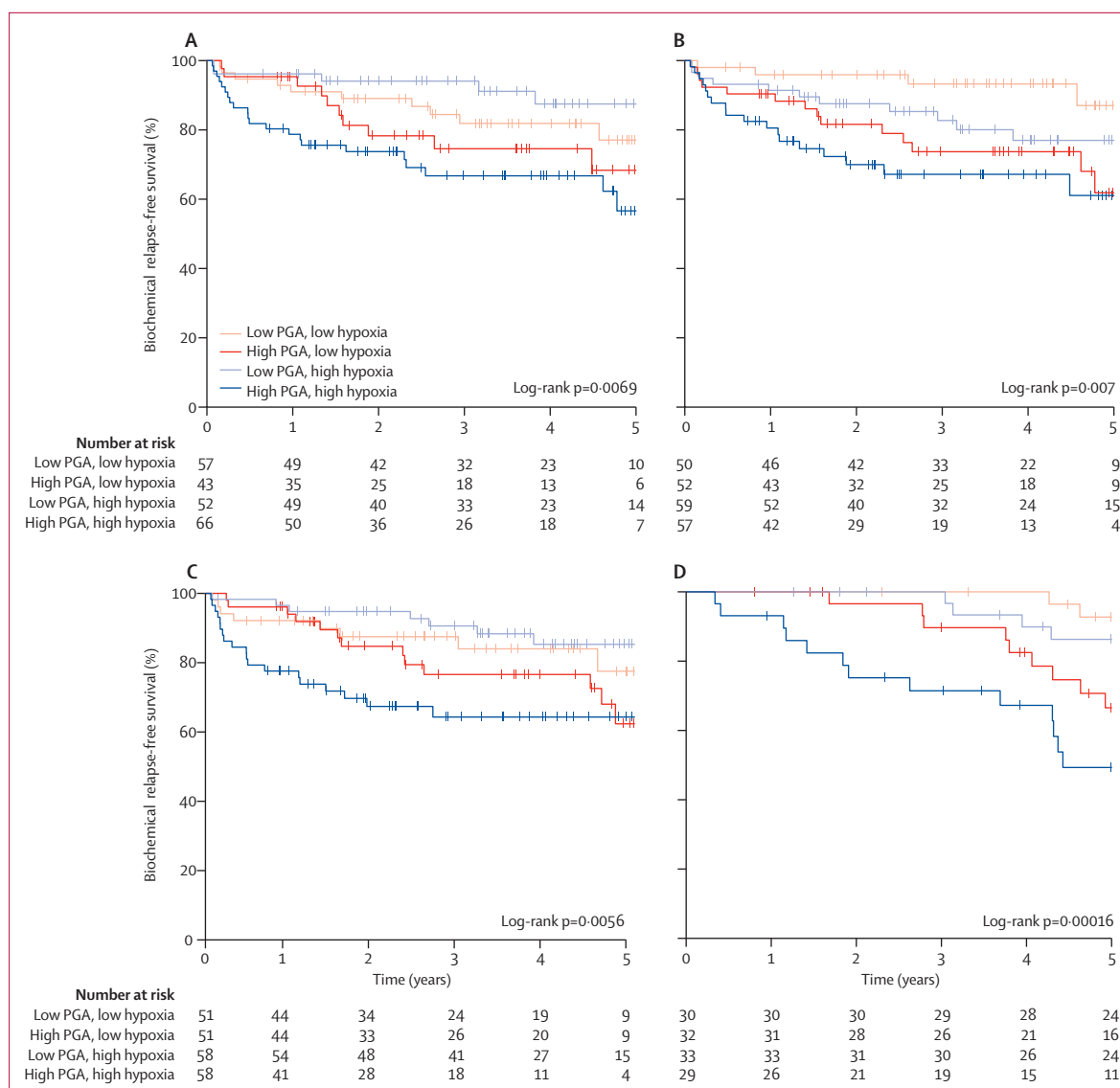


**Figure 4: Kaplan-Meier analysis of biochemical relapse for patients stratified by PGA and hypoxia values**

Combining genome instability (PGA) and hypoxia within the same patient has an additive and independent prognostic effect when tumour hypoxia is measured with the Buffa (A), West (B), or Winter RNA signatures (C) in the pooled radical prostatectomy full cohorts (n=271). When genomic instability (PGA) and hypoxia (HP20) were combined within the same patient, we noted a multiplicative and independent prognostic effect in image-guided radiotherapy patients (D). HP20=proportion of oxygen measurements less than 20 mm Hg.

p=0.021) and was highly prognostic for low-risk patients (AUC 0.97 [95% CI 0.82–1.0]; appendix pp 71–75). Importantly, the signature also identified patients who go on to develop metastasis (AUC 0.78 [95% CI 0.63–0.93]; appendix p 76).

To underpin the potential use of our DNA signature, we noted that the signature had AUC and C-index values that were greater than 97% (970 000/1 000 000) of the empirical null distribution from randomly sampled genesets (appendix p 77). Furthermore, our signature outperformed 23 previously published RNA signatures for prostate cancer biochemical relapse-free survival rates after training of random forests with a

cohort of 1299 low-risk to high-risk patients with prostate cancer (including 293 low-risk to intermediate-risk patients) with mRNA microarray data (figure 6). Application of these trained forests to the 108 MSKCC patients with information about both mRNA and copy number alteration showed that our DNA signature has the highest overall AUC (figure 6A, B; appendix pp 31, 78).

There is a low alteration rate for most of the genes identified in the signature: 154 (56%) of 276 genes had copy-number alterations in zero to 39 patients (of a total sample size of 397 patients), which is less than 10% of the total combined cohorts size (appendix p 79).

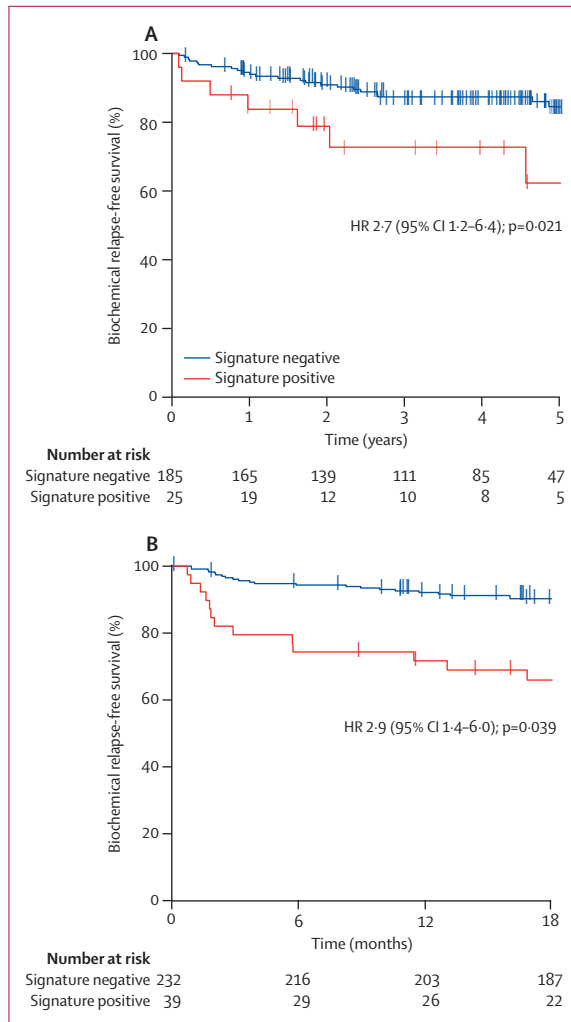


**Figure 5: A prognostic DNA signature for prostate cancer**  
 Multivariate Cox proportional hazard model adjusting for clinical covariates (Gleason score and pretreatment PSA) in the low-risk and intermediate-risk groups (A) and when applied to the full pooled radical prostatectomy cohort (n=271) the signature for copy number alteration identifies patients who will fail rapidly (B). HR=hazard ratio. Signature positive=patients whose tumour genomics were positive for the 100-loci DNA. Signature negative=patients whose tumour genomics were negative for the DNA signature.

These results strongly support the use of multigene models, because our biopsy-based DNA signature outperformed reported prognostic genes (appendix p 80). Signature regions are distributed across 14 chromosomes and range by an order of magnitude in their importance to prediction accuracy (appendix p 81). Notably, genes in these regions relate to lipid metabolism (appendix p 82).

We noted that the signature directly accounts for genomic instability (appendix pp 82–85). First, patients with subtype-4 tumours have significantly lower signature risk scores than do those with other subtypes (median 0.17 [IQR 0.0026–0.32] vs 0.41 [0.31–0.61];  $p < 0.0001$ , two-sided Mann-Whitney *U* test). Second, percentage of genome alteration differs significantly between the classes predicted by the signature and can be estimated from the gene signature (Spearman’s correlation between whole-genome and signature-estimated percentage of genome alteration  $\rho = 0.73$ ;  $p < 0.0001$ ), thereby providing similar prognostic information. Importantly, signature-based estimates of percentage of alteration remain highly prognostic, and the addition of 30 genes (selected from the Toronto cohort) improves estimates of percentage of alteration in the validation cohorts (eg, MSKCC: Spearman’s  $\rho = 0.73$  vs 0.87;  $p < 0.0001$ ; appendix p 32). The HR of percentage of genome alteration as a continuous variable estimated from these 306 genes is identical to that of the true percentage of genome alteration in the MSKCC cohort and nearly identical to that of the Cambridge cohort. Taken together, these results show that our treatment-independent DNA-prognostic signature measures genomic instability in addition to lipid metabolism pathways, suggesting our signature might identify candidates for treatment-intensification trials targeting these processes (appendix pp 86–91).

### Discussion

Our findings show that combined indices of genomic instability and hypoxia can improve accuracy of prognosis in patients with localised prostate cancer in the context of present clinicopathological variables. Development of prostate-cancer biomarkers to guide disease management at the time of diagnosis is a difficult but crucial challenge in view of the high rates of overtreatment and clinical relapse.<sup>30</sup> Initial investigation in the Toronto cohort showed striking genomic heterogeneity in the pre-treatment biopsies from these patients, and has implications for the discovery of driver mutations in prostate cancer. No copy number alterations were recurrent in more than 47% of patients and the number of alterations per patient ranged from zero to 187. We were, however, able to identify independent molecular prognostic subtypes based on genome-wide copy number alteration profiles in the Toronto cohort.

Inclusion of additional patients from the independent MSKCC cohort of low-risk and intermediate-risk patients

	MSKCC full cohort		Cambridge full cohort*	
	Univariate	Multivariate	Univariate	Multivariate
100-loci DNA signature	4.0 (2.0–8.1; 0.00011)	2.8 (1.4–6.0; 0.0060)	2.9 (1.1–8.2; 0.038)	2.9 (1.0–8.2; 0.050)
AUC	0.74 (0.68–0.80)	0.84 (0.78–0.89)	0.64 (0.57–0.71)	0.75 (0.68–0.83)
C index	0.70 (0.61–0.80)	0.74 (0.65–0.83)	0.67 (0.54–0.79)	0.73 (0.62–0.85)

Data are hazard ratio (95% CI; p value) or hazard ratio (95% CI). Data are provided for the 100-loci DNA signature in each full validation cohort on the basis of Cox proportional hazard models including only the marker of interest (univariate) and models including relevant clinical covariates as in the multivariate models in table 1 (multivariate). The AUC and C index are provided for the continuous signature risk score. MSKCC=Memorial Sloan Kettering Cancer Center. AUC=area under the receiver operator curve. \*Data are based on 18-month biochemical recurrence.

**Table 4: Performance of the 100-loci DNA signature**



led to larger subtype sizes amenable to analyses of biochemical relapse-free survival, showing significant differences in patient outcome according to subtype. Patients flagged by our copy-number alteration-based signature had biochemical relapse rates that were increased by up to six times, and were at risk of failure within 18 months, all within the clinical context of Gleason score, T category, and PSA. In particular, this signature is highly effective for low-risk patients, because it can identify those ineligible for active surveillance and provide additional assurance for those who are. For instance, if the DNA signature was used by clinicians today, of 1000 patients diagnosed with localised disease, 144 patients would be offered more aggressive treatment (all signature-positive patients) and 650 would have the support for active surveillance instead of local treatment (low-risk to intermediate-risk signature-negative patients).

Preclinical experimental work supports hypoxia generating a mutator phenotype (decreased DNA repair leading to increased mutation rate and genomic instability) and selecting for genetically unstable clones, in addition to an increased capacity for distant metastases.<sup>18</sup> This metastatic phenotype occurs independently of local treatment; hypoxia is associated with both local relapse after image-guided radiotherapy and biochemical failure and distant metastasis in patients receiving image-guided radiotherapy or radical prostatectomy for prostate cancer.<sup>19,20</sup> Here we have shown that simultaneous measurement of tumour hypoxia and genomic instability can improve the prognostic capability of a pretreatment biopsy by combining the independent biology of cancer genomics with the tumour microenvironment. Moreover, the poor prognosis previously associated with hypoxia<sup>19,20</sup> might have been related to genomic instability within a subset of these specimens, because hypoxia itself was not associated with poor prognosis in the absence of a heightened percentage of genome alteration.

Cancer-cell metabolism (increased glycolysis, high lactate, and hypoxia) is related to oncogene activation and loss of tumour suppressor genes, and increased lipid and fatty acid synthesis have been associated with progression of prostate cancer.<sup>31,32</sup> Therefore it is striking that our supervised machine-learning approach led to the discovery of a genetic signature enriched for genes involved in lipid biology. Combined with the finding that constitutive activation of mTORC1 renders hypoxic cells dependent on exogenous desaturated lipids, our signature could represent abnormalities in cancer metabolism amenable to targeting of lipid synthesis.<sup>31–34</sup> Furthermore, our signature efficiently captures the prognostic effect of percentage of genome alteration—a surrogate for genomic instability. Because androgen deprivation therapy improves oxygenation<sup>35</sup> and reduces DNA repair<sup>36</sup> in patients with prostate cancer, we speculate that such therapies targeting hypoxia and

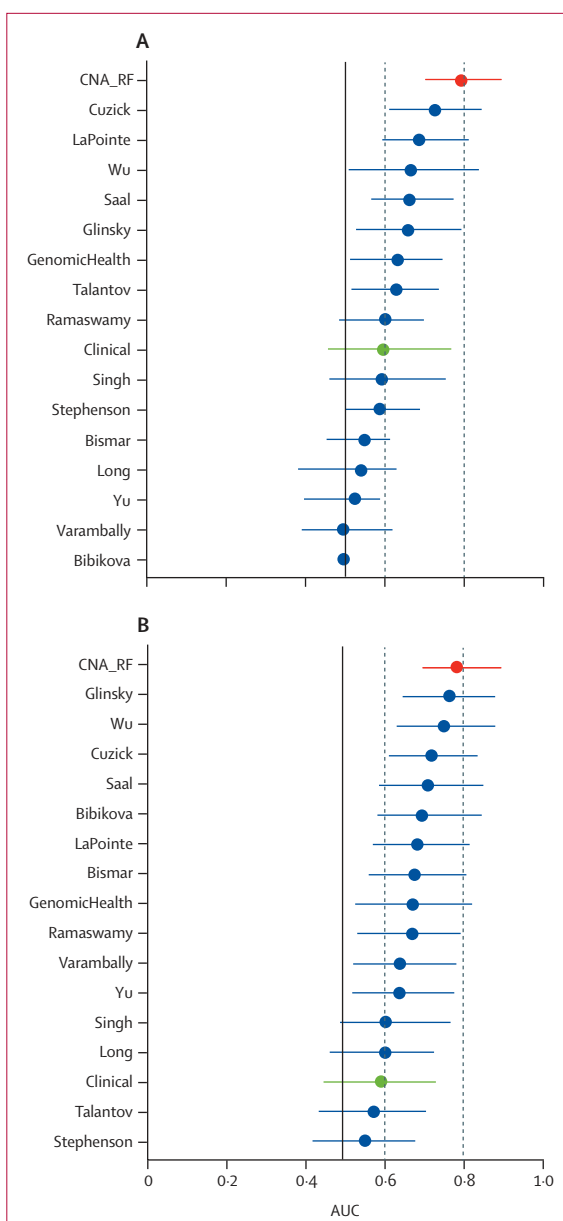


**Figure 6: Training and comparison of random forest signatures for 23 previously published RNA signatures for biochemical relapse-free survival** We trained a clinical model (in green) with clinical variables: pretreatment PSA, biopsy-based Gleason score, and T category. We compared our DNA-based signature (CNA\_RF, shown in red) with these signatures in the 108 Memorial Sloan Kettering Cancer Center patients with information about both mRNA and CNA. The DNA, RNA, and clinical signatures were trained in a cohort of 293 low-risk to intermediate-risk patients with prostate cancer (A) and 1299 low-risk to high-risk patients (B), including some with locally advanced disease. In cases where more than one study published more than one signature, only the best performing signature is shown. CNA=copy number alterations. AUC=area under the receiver operator curve.

genomic instability might be effective in prevention of clinical relapse. Patients flagged by our signature might benefit from patient-specific intensification with androgen deprivation therapy or other systemic therapies

to offset both local and systemic resistance, independent of primary treatment.

To our knowledge, this is the first report of biopsy-driven, DNA-based indices that predicts prognosis in patients who received either image-guided radiotherapy or radical prostatectomy as primary therapy for patients with prostate cancer (panel). DNA alterations might be less variable than RNA abundance patterns within intraprostatic biopsies from dynamic tumour microenvironments, and more stable *ex vivo* during formalin-fixed, paraffin-embedded protocols. This finding suggests that our DNA signatures are robust for clinical application. Because our training cohort was obtained before primary therapy, our study supports the characterisation of complex indices, showing *a priori* interpatient heterogeneity, soon after diagnostic MRI-guided or transurethral ultrasound-guided biopsies. Indeed, we have shown that frozen biopsies are amenable to whole-genome sequencing to assess intrapatient heterogeneity in genomic aberrations (Boutros PC, unpublished).

Our study has several caveats. Use of biochemical relapse as an endpoint is suboptimum compared with prostate cancer-specific mortality or time to metastasis. Nonetheless, our signature shows promise in identification of patients with metastasis, and can identify patients who will have biochemical relapse before 18 months, which has been shown to be predictive for prostate cancer-specific mortality.<sup>6,7</sup> Although the cohorts

differ slightly in the distribution of clinicopathological factors, these differences changed neither treatment nor survival, making it very unlikely that the differences affect the interpretation of our results. Nevertheless, we did systematically stratify our analyses according to these factors when we assessed prognostic markers. A subset of patients were given adjuvant treatment; however, we do not yet know how adjuvant treatment affects the performance of our signature. We will explore this outcome in new cohorts of patients treated with image-guided radiotherapy or radical prostatectomy with or without androgen deprivation therapy, and assess whether the biomarker would become a predictive, rather than a solely prognostic, biomarker.

From a technical perspective, despite different resolutions between the copy number alteration platforms used for each cohort, the copy number alteration indices developed in the Toronto cohort validated in the radical prostatectomy cohorts. The hypoxia probes measure global hypoxia within a prostate-cancer locale, but do not measure intracellular hypoxia. As a result, the DNA is obtained from a large region relative to sites of hypoxia. In future studies we will characterise the DNA, RNA, and epigenetic profiles of foci within patients who receive oral pimonidazole before treatment to investigate the genomic-hypoxia prognostic association in finer detail. Finally, efforts are underway to reduce the signature size without loss of prognostic information related to metabolism or genomic instability, and to improve the sensitivity of our signature with multimodal data sets (eg, combined DNA, RNA and epigenetic analyses) emerging from studies from the International Cancer Genome Consortium and The Cancer Genome Atlas.

Identification of the correct patients to treat while avoiding overtreatment in the low-risk to intermediate-risk group remains an important clinical dilemma. We envision the use of genomic instability and microenvironment signatures to divert patients from present clinical risk categories to novel clinical trials of treatment intensification, whereby patients with poor prognosis based on these novel biomarkers can be enrolled into trials that add combined local and systemic therapies. Additionally, low-risk and intermediate-risk patients with low levels of hypoxia and and low percentages of genome alteration could be entered into clinical trials of active surveillance. These precision medicine approaches set the stage for novel treatment intensification and treatment deintensification trials to either increase cure rates by prevention of progression to metastatic castration-resistant prostate cancer or to reduce the burden of overtreatment.

#### Contributors

EL contributed to the bioinformatics analysis, machine learning, the statistical analysis, visualisation, and manuscript preparation. ASI contributed to analysis of the percentage of genome alteration and manuscript preparation. JS contributed to the statistical analysis and clinical trial design. MF contributed to the study design and

#### Panel: Research in context

##### Systematic review

We reviewed previous studies on the basis of PubMed searches done between Jan 1, 1990, and Dec 31, 2013, with the terms: "genomics", "DNA", "RNA", "hypoxia", "prognosis", "radiotherapy", "surgery", "radical prostatectomy", "aCGH", "RNA expression", "arrays", "classifier", and "biomarker". We focused on multigene indices that had been validated in at least one cohort, and noted many previously published RNA signatures for prognosis in prostate cancer and for hypoxia in various tissue types. To the best of our knowledge, no multigene DNA signature exists, and no biomarker assesses genomics and the tumour microenvironment simultaneously.

##### Interpretation

We propose the use of DNA-based and RNA-based signatures to measure genomic instability and tumour hypoxia to guide clinical management of patients with primary diagnostic biopsies. Our 100-loci DNA signature, which measures genomic instability and is enriched for lipid metabolism genes, outperforms previously published RNA-based prognostic signatures for prostate cancer. Once our assays undergo clinical quality assurance protocols within a hospital setting, clinicians can use this assay to divert patients to appropriate clinical trials.

manuscript preparation. HR-A contributed to the study design, sample processing, and clinical annotation for the Cambridge cohort. NE, LLL, and ED did the RNA signature comparison. MJD and SH undertook pre-processing and development of copy number alterations for the Cambridge cohort. ADL contributed to study design and clinical annotation for the Cambridge cohort. NCM and NJH contributed to the statistical analysis. GZ did the sample preparation for the image-guided radiotherapy cohort. AYW was responsible for histopathology of the Cambridge cohort. XM did tissue processing for the image-guided radiotherapy cohort. JT contributed to clinical annotation for the image-guided radiotherapy cohort. MRG and HX did the signature permutation analysis. AB contributed to clinical analysis, trial design, and manuscript preparation. CLH undertook initial validation of aCGH data for the image-guided radiotherapy cohort. VRR contributed to bioinformatics and aCGH analysis for the image-guided radiotherapy cohort. CQY did the pathway analysis. CAM contributed to sample preparation for the image-guided radiotherapy cohort. DYFM contributed to bioinformatics analysis and data preprocessing. KCC contributed to the statistical analysis and bioinformatics analysis. LCC contributed to bioinformatics analysis (visualisation support). DHS contributed to bioinformatics analysis and data processing for the Memorial Sloan Kettering Cancer Center cohort. CP designed the figures. CCC, CC, and RE contributed to the study design. JAS contributed to study design and did FISH validation. IJ contributed to bioinformatics analysis. MP did the statistical design. ADP did clinical analysis. MM did the hypoxia analysis and contributed to study design. DEN contributed to study design and was the lead scientist responsible for the Cambridge cohort and its molecular profiling. TvdK undertook pathological analysis and contributed to the study design. PCB contributed to study design, bioinformatics and statistical analyses, and manuscript preparation. RGB contributed to study design, clinical analysis, and manuscript preparation

#### Declaration of interest

EL, PCB, and RGB have a patent “Biopsy-driven genomic signature for prostate cancer prognosis” pending. NE, LLL, and ED are employees of GenomeDx Biosciences and report personal fees from GenomeDx Biosciences during the conduct of the study. NE, LLL, and ED have a patent “Cancer Diagnostics Using Biomarkers” pending. NE and LLL have a patent “Cancer diagnostics using non-coding transcripts” pending. LLL has a patent “Bladder Cancer Diagnostics” pending, and ED has a patent “Systems and Methods for Expression-Based Discrimination of Distinct Clinical Disease States in Prostate Cancer” pending. CCC has a patent “Biomarkers for prostate cancer metastasis” issued (number 7482123; 2009). All other authors have no competing interests.

#### Acknowledgments

We thank study volunteers for their participation, and staff at the Wellcome Trust Clinical Research Facility, Addenbrooke's Clinical Research Centre, Cambridge, UK for their help in conducting the study. This study was done with the support of Movember funds through Prostate Cancer Canada and with the additional support of the Ontario Institute for Cancer Research, funded by the Government of Ontario and by a Doctoral Fellowship from the Canadian Institute for Health Research to EL. We acknowledge the support of the National Institutes of Health Research Cambridge Biomedical Research Centre and the National Cancer Research Prostate Cancer: Mechanisms of Progression and Treatment (ProMPT) collaborative (grant code G0500966/75466), which has funded tissue and urine collections in Cambridge. We acknowledge the support of The University of Cambridge, Cancer Research UK and Hutchison Whampoa Limited, and the support of Cancer Research UK Cambridge Institute Genomics and Bioinformatics core facilities. This work was funded in part by a Cancer Research UK programme grant awarded to DEN. PCB was supported by a Terry Fox Research Institute New Investigator Award, a CIHR New Investigator Award. This study was supported by Prostate Cancer Canada and is funded by the Movember Foundation (grant number RS2014-01). We thank the Princess Margaret Cancer Centre Foundation, the PMH-Radiation Medicine Program Academic Enrichment Fund, and Motorcycle Ride for Dad (Durham) for support. RGB is a recipient of a Canadian Cancer Society Research Scientist Award.

#### References

- 1 Ferlay J, Shin HR, Bray F, Forman D, Mathers C, Parkin DM. Estimates of worldwide burden of cancer in 2008: GLOBOCAN 2008. *Int J Cancer* 2010; **127**: 2893–917.
- 2 D'Amico AV, Moul J, Carroll PR, Sun L, Lubeck D, Chen MH. Cancer-specific mortality after surgery or radiation for patients with clinically localized prostate cancer managed during the PSA era. *J Clin Oncol* 2003; **21**: 2163–72.
- 3 Mohler JL. The 2010 NCCN clinical practice guidelines in oncology on prostate cancer. *J Natl Compr Canc Netw* 2010; **8**: 145.
- 4 Shao YH, Demissie K, Shih W, et al. Contemporary risk profile of prostate cancer in the United States. *J Natl Cancer Inst* 2009; **101**: 1280–83.
- 5 Nichol AM, Warde P, Bristow RG. Optimal treatment of intermediate-risk prostate carcinoma with radiotherapy: clinical and translational issues. *Cancer* 2005; **104**: 891–905.
- 6 Freedland SJ, Humphreys EB, Mangold LA, et al. Risk of prostate cancer-specific mortality following biochemical recurrence after radical prostatectomy. *JAMA* 2005; **294**: 433–39.
- 7 Buyyounouski MK, Pickles T, Kestin LL, Allison R, Williams SG. Validating the interval to biochemical failure for the identification of potentially lethal prostate cancer. *J Clin Oncol* 2012; **30**: 1857–63.
- 8 Taylor BS, Schultz N, Hieronymus H, et al. Integrative genomic profiling of human prostate cancer. *Cancer cell* 2010; **18**: 11–22.
- 9 Lunt SJ, Chaudary N, Hill RP. The tumor microenvironment and metastatic disease. *Clin Exp Metastasis* 2009; **26**: 19–34.
- 10 Saylor PJ, Smith MR. Metabolic complications of androgen deprivation therapy for prostate cancer. *J Urol* 2009; **181**: 1998–2008.
- 11 Shen MM, Abate-Shen C. Molecular genetics of prostate cancer: new prospects for old challenges. *Genes Dev* 2010; **24**: 1967–2000.
- 12 Locke JA, Zafarana G, Malloff CA, et al. Allelic loss of the loci containing the androgen synthesis gene, StAR, is prognostic for relapse in intermediate-risk prostate cancer. *Prostate* 2012; **72**: 1295–305.
- 13 Cuzick J, Swanson GP, Fisher G, et al. Prognostic value of an RNA expression signature derived from cell cycle proliferation genes in patients with prostate cancer: a retrospective study. *Lancet Oncol* 2011; **12**: 245–55.
- 14 Wu CL, Schroeder BE, Ma XJ, et al. Development and validation of a 32-gene prognostic index for prostate cancer progression. *Proc Natl Acad Sci USA* 2013; **110**: 6121–26.
- 15 Erho N, Crisan A, Vergara IA, et al. Discovery and validation of a prostate cancer genomic classifier that predicts early metastasis following radical prostatectomy. *PLoS One* 2013; **8**: e66855.
- 16 Minner S, Enodien M, Sirma H, et al. ERG status is unrelated to PSA recurrence in radically operated prostate cancer in the absence of antihormonal therapy. *Clin Cancer Res* 2011; **17**: 5878–88.
- 17 Dal Pra A, Lalonde E, Sykes J, et al. TMPRSS2-ERG status is not prognostic following prostate cancer radiotherapy: implications for fusion status and DSB repair. *Clin Cancer Res* 2013; **19**: 5202–09.
- 18 Bristow RG, Hill RP. Hypoxia, DNA repair and genetic instability. *Nat Rev Cancer* 2008; **8**: 180–92.
- 19 Vergis R, Corbishley CM, Norman AR, et al. Intrinsic markers of tumour hypoxia and angiogenesis in localised prostate cancer and outcome of radical treatment: a retrospective analysis of two randomised radiotherapy trials and one surgical cohort study. *Lancet Oncol* 2008; **9**: 342–51.
- 20 Milosevic M, Warde P, Menard C, et al. Tumor hypoxia predicts biochemical failure following radiotherapy for clinically localized prostate cancer. *Clin Cancer Res* 2012; **18**: 2108–14.
- 21 Breiman L. Random Forest. *Machine Learning* 2001; **45**: 5–32.
- 22 Roach M, Hanks G, Thames HJ, et al. Defining biochemical failure following radiotherapy with or without hormonal therapy in men with clinically localized prostate cancer: recommendations of the RTOG-ASTRO Phoenix Consensus Conference. *Int J Radiat Oncol Biol Phys* 2006; **65**: 965–74.
- 23 Mottet N, Bastian PJ, Bellmunt J, et al. Guidelines on prostate cancer. April, 2014. [http://www.uroweb.org/gls/pdf/09%20Prostate%20Cancer\\_LRLV2.pdf](http://www.uroweb.org/gls/pdf/09%20Prostate%20Cancer_LRLV2.pdf) (accessed June 20, 2014).
- 24 Liu W, Chang BL, Cramer S, et al. Deletion of a small consensus region at 6q15, including the MAP3K7 gene, is significantly associated with high-grade prostate cancers. *Clin Cancer Res* 2007; **13**: 5028–33.

- 25 Baca SC, Prandi D, Lawrence MS, et al. Punctuated evolution of prostate cancer genomes. *Cell* 2013; **153**: 666–77.
- 26 Hieronymus H, Schultz N, Gopalan A, et al. Copy number alteration burden predicts prostate cancer relapse. *Proc Natl Acad Sci USA* 2014; **110**: 11139–44.
- 27 Buffa FM, Harris AL, West CM, Miller CJ. Large meta-analysis of multiple cancers reveals a common, compact and highly prognostic hypoxia metagene. *Br J Cancer* 2010; **102**: 428–35.
- 28 Winter SC, Buffa FM, Silva P, et al. Relation of a hypoxia metagene derived from head and neck cancer to prognosis of multiple cancers. *Cancer Res* 2007; **67**: 3441–49.
- 29 Eustace A, Mani N, Span PN, et al. A 26-Gene Hypoxia Signature Predicts Benefit from Hypoxia-Modifying Therapy in Laryngeal Cancer but Not Bladder Cancer. *Clin Cancer Res* 2013; **19**: 4879–88.
- 30 Prensner JR, Rubin MA, Wei JT, Chinnaiyan AM. Beyond PSA: the next generation of prostate cancer biomarkers. *Sci Transl Med* 2012; **4**: 127rv3.
- 31 Fritz V, Benfodda Z, Henriquet C, et al. Metabolic intervention on lipid synthesis converging pathways abrogates prostate cancer growth. *Oncogene* 2013; **32**: 5101–10.
- 32 Yue S, Li J, Lee S-Y, et al. Cholesteryl ester accumulation induced by PTEN Loss and PI3K/AKT activation underlies human prostate cancer aggressiveness. *Cell Metab* 2014; **19**: 393–406.
- 33 Young RM, Ackerman D, Quinn ZL, et al. Dysregulated mTORC1 renders cells critically dependent on desaturated lipids for survival under tumor-like stress. *Genes Dev* 2013; **27**: 1115–31.
- 34 Menon S, Manning BD. Common corruption of the mTOR signaling network in human tumors. *Oncogene* 2008; **27**: S43–51.
- 35 Milosevic M, Chung P, Parker C, et al. Androgen withdrawal in patients reduces prostate cancer hypoxia: implications for disease progression and radiation response. *Cancer Res* 2007; **67**: 6022–25.
- 36 Goodwin JF, Schiewer MJ, Dean JL, et al. A hormone-DNA repair circuit governs the response to genotoxic insult. *Cancer Discov* 2013; **3**: 1254–71.